New Phytologist

Light acclimation in the lycophyte *Selaginella martensii* depends on changes in the amount of photosystems and on the flexibility of the light-harvesting complex II antenna association with both photosystems

Lorenzo Ferroni[1], Marjaana Suorsa[2], Eva-Mari Aro[2], Costanza Baldisserotto[1] and Simonetta Pancaldi[1]

[1]Department of Life Sciences and Biotechnology, University of Ferrara, C.so Ercole I d'Este 32, 44121 Ferrara, Italy; [2]Department of Biochemistry, Molecular Plant Biology, University of Turku, FI-20014 Turku, Finland

Author for correspondence:
Lorenzo Ferroni
Tel: +39 0532293779
Email: lorenzo.ferroni@unife.it

Received: *15 September 2015*
Accepted: *20 February 2016*

New Phytologist (2016) **211:** 554–568
doi: 10.1111/nph.13939

Key words: chlorophyll fluorescence, light acclimation, light-harvesting complex, lycophytes, native gel electrophoresis, photosystem, *Selaginella martensii*, thylakoid membrane.

Summary

• Vascular plants have evolved a long-term light acclimation strategy primarily relying on the regulation of the relative amounts of light-harvesting complex II (LHCII) and of the two photosystems, photosystem I (PSI) and photosystem II (PSII). We investigated whether such a model is also valid in *Selaginella martensii*, a species belonging to the early diverging group of lycophytes.

• *Selaginella martensii* plants were acclimated to three natural light regimes (extremely low light (L), medium light (M) and full sunlight (H)) and thylakoid organization was characterized combining ultrastructural, biochemical and functional methods.

• From L to H plants, thylakoid architecture was rearranged from (pseudo)lamellar to predominantly granal, the PSII : PSI ratio changed in favour of PSI, and the photochemical capacity increased. However, regulation of light harvesting did not occur through variations in the amount of free LHCII, but rather resulted from the flexibility of the association of free LHCII with PSII and PSI.

• In lycophytes, the free interspersed LHCII serves a fixed proportion of reaction centres, either PSII or PSI, and the regulation of PSI–LHCII(–PSII) megacomplexes is an integral part of long-term acclimation. Free LHCII ensures photoprotection of PSII, allows regulated use of PSI as an energy quencher, and can also quench endangered PSI.

Introduction

The success of vascular plants under the diverse light environments in land habitats has been correlated with the evolution of grana–intergrana thylakoid differentiation inside the chloroplast (Anderson *et al.*, 2012), which is the expression of so-called 'lateral heterogeneity' (Andersson & Anderson, 1980). Photosystem II (PSII), with its chlorophyll (Chl) *a*/*b*-containing light-harvesting complex LHCII, is mainly located in the stacked domains, while photosystem I (PSI), LHCI and ATP synthase are confined to the stroma-exposed regions. Cytochrome b_6f (Cytb_6f) mediates electron transport from PSII to PSI, transferring electrons from reduced plastoquinone (PQ) to plastocyanin, and is enriched in stroma-exposed membranes (Armbruster *et al.*, 2013; Wunder *et al.*, 2013; Grieco *et al.*, 2015). Some auxiliary thylakoid proteins have also been assigned to different thylakoid domains; for example, the PSII subunit S (PsbS), a key regulatory protein in nonphotochemical quenching (NPQ; Wilk *et al.*, 2013), resides in grana membranes, while proteins involved in PSII repair are enriched in stroma-exposed domains (Suorsa *et al.*, 2014).

Starting from a complete absence of lateral heterogeneity in the Chl*b*-containing algae Prasinophyceae (Song & Gibbs, 1995), grana–intergrana differentiation was gradually refined in the green lineage (Gunning & Schwartz, 1999). However, the main evolutionary forces that drove grana evolution still remain elusive. It has been suggested that enhancement of light harvesting, prevention of PSII-to-PSI energy spillover, spatial separation of cyclic electron transport from linear electron transport or better regulation of PSII turnover has facilitated differentiation of grana and the subsequent lateral heterogeneity (Nevo *et al.*, 2012; Pribil *et al.*, 2014). Evolution of thylakoid organization in the green lineage up to vascular plants has also influenced regulation of photosynthetic mechanisms (Grouneva *et al.*, 2013). The dynamic structure of the thylakoid system allows vascular plants to cope with fluctuating irradiance (Anderson *et al.*, 2012). Short-term mechanisms include dissipation of excess of light energy (qE), regulation of excitation energy distribution between PSI and PSII, the PSII repair cycle, and fine-tuning of electron transport via alternative electron acceptors, such as plastoquinol terminal oxidase (PTOX; for

reviews, see Demmig-Adams *et al.*, 2012; Tikkanen & Aro, 2014; Goldschmidt-Clermont & Bassi, 2015; Järvi *et al.*, 2015; Tikhonov, 2015). Long-term acclimation to natural light regimes relies primarily on two types of adjustment, namely, changes in (1) the relative amount of LHCII, resulting in changes in the Chl*a*:*b* ratio, and (2) the PSI : PSII ratio, which is modulated in favour of the less excited photosystem (Walters & Horton, 1994; Murchie & Horton, 1998; Lichtenthaler & Babani, 2004). Because shade-acclimated plants are limited in light harvesting, they have more LHCII relative to PSII and, correspondingly, low Chl*a*:*b* values (2.3–2.7); moreover, the understory enrichment in far red light is balanced by a lower PSI : PSII ratio (Lichtenthaler & Babani, 2004; Hogewoning *et al.*, 2012). Conversely, less LHCII, a high Chl*a*:*b* ratio (3–4.5) and a high PSI : PSII ratio characterize sun-acclimated plants, which prioritize energy conversion capacity and photoprotection ability (Anderson *et al.*, 1988; Lichtenthaler & Babani, 2004; Ballottari *et al.*, 2007). Changes in LHCII/photosystem stoichiometry upon sun/shade acclimation are mirrored in well-known variations of thylakoid architecture, shade plants indeed having more appressed thylakoids relative to nonappressed thylakoids than sun plants. To what extent such variations are linked to the supramolecular organization of the complexes is unclear. In angiosperms, low-light acclimation causes accumulation of LHCII trimers not stably bound to PSII (Pantaleoni *et al.*, 2009; Kouřil *et al.*, 2013; Ware *et al.*, 2015). However, the function of these free LHCII trimers, also called 'extra LHCII' (Kouřil *et al.*, 2013), is still largely unknown. According to a 'lake model' organization of PSII units, the free LHCII interspersed between PSII units in grana stacks should enhance the efficiency of light harvesting (Kramer *et al.*, 2004).

Tracing back the evolution of sun/shade acclimation in the green lineage is challenging. Modulability of the PSII antenna size has been documented in various green microalgae (e.g. Maxwell *et al.*, 1995; Webb & Melis, 1995; Teramoto *et al.*, 2002). In the marine macroalgae Ulvophyceae, the Chl*a*:*b* ratio was found to be similar to that of extreme shade land plants (Yamazaki *et al.*, 2005) and could undergo long-term light-driven regulation (Bischof *et al.*, 2006). Bryophytes, the simplest, nonvascular extant land plants, can modulate thylakoid stacking and carotenoid complement, but lack flexibility in the Chl*a*:*b* ratio (Aro, 1982; Marschall & Proctor, 2004; Gerotto *et al.*, 2011). A certain ability to modulate the antenna size occurs in rainforest ferns, with Chl*a*:*b* varying in the range of 1.8–2.9 (Nasrulhaq-Boyce & Haji, 1987; Nasrulhaq-Boyce & Duckett, 1991). Fossil forests of lycophytes suggest that ancestral vascular plants must have been capable of acclimation to light regimes ranging from full sunlight to shade. Lycophytes, as early diverging vascular plants, offer a rare opportunity to investigate the evolution of the photosynthetic mechanisms that emerged upon acclimation to land habitats (Ferroni *et al.*, 2014). In this study, we investigated whether the thylakoid organization that sustains long-term light acclimation (low light, medium light and full sunlight) in the lycophyte *Selaginella martensii* is consistent with the current models of thylakoid photoregulation in vascular plants.

Materials and Methods

Plant material

Selaginella martensii Spring (Selaginellaceae) was cultivated in a humid glasshouse of the Botanical Garden of Ferrara (Italy) at 25–30°C. The medium light (M) condition corresponded to the natural light regime which is usual for this species in the glasshouse. Shading by plants growing above gave a daily peak of the photosynthetic photon fluence rate (PPFR) of *c.* 50 μmol m^{-2} s^{-1} over a spectrum of 400–700 nm. For long-term acclimation, some plants were transferred to extremely low light, under the shade of broadleaved plants (L; *c.* 5 μmol m^{-2} s^{-1}), or to direct sunlight (H; *c.* 1500 μmol m^{-2} s^{-1}). Supporting information Fig. S1 exemplifies the daily light regimes. Experiments were performed between March and October in 2010–2014. All analyses focussed on terminal branches of plants light-acclimated for at least 3 wk to each condition.

Electron microscopy

Small segments of terminal branches were fixed with 3% glutaraldehyde in 0.1 M Na-K phosphate buffer (pH 7.2) for 4 h at 4°C. After overnight post-fixation with 1% OsO_4 in the same buffer, routine protocols for dehydration, embedding and staining were applied (Baldisserotto *et al.*, 2007). Ultrathin sections were observed with a Hitachi H800 electron microscope (at the Electron Microscopy Centre, University of Ferrara).

Photosynthetic pigment analyses

Photosynthetic pigments were extracted with 100% methanol at 80°C for 10 min and extracts were analysed spectrophotometrically for pigment quantification (Wellburn, 1994).

Thylakoid isolation

Branches were sampled after 12 h of darkness or 1 h of light exposure (1000 μmol m^{-2} s^{-1}) using a halogen lamp screened with 4 cm of water. Branches were ground in an ice-cold mortar for 1 min and thylakoid isolation was performed essentially according to Järvi *et al.* (2011). Thylakoids were rapidly frozen in liquid nitrogen and stored at −80°C. Chl content was determined after extraction with 80% (v/v) acetone (Porra *et al.*, 1989).

SDS-PAGE and immunoblotting

Thylakoid proteins were separated by SDS-PAGE on a 15% acrylamide, 6 M urea resolving gel (Laemmli, 1970). Proteins were stained with the quantitative, highly sensitive dye SYPRO® Ruby (Invitrogen; Lopez *et al.*, 2000) and imaged at five different exposure times with a Geliance 1000 Imaging System (Perkin-Elmer). Alternatively, they were electroblotted onto a polyvinylidene difluoride membrane (Millipore) for immunodetection. Western blotting with specific antibodies and detection with

enhanced chemiluminescence were performed following standard protocols. Chl*a*-binding CP47 subunit of PSII (CP47), LHCII, PSI and PsbS antibodies were kindly provided by R. Barbato, NAD(P)H dehydrogenase-like complex subunit H (NdhH) antibody by D. Rumeau, and ferredoxin-$NADP^+$ oxido-reductase (FNR) antibody by H. V. Scheller. Lhcb6, Cyt*f* and ATP-β antibodies were purchased from Agrisera (Vännäs, Sweden; product codes AS01010, AS06119 and AS05085, respectively).

Nondenaturing large-pore blue native polyacrylamide gel electrophoresis (lpBN-PAGE)

Thylakoids were solubilized in darkness at a final Chl concentration of 0.5 mg ml^{-1} with 1.5% (w/v) β-dodecylmaltoside (DM) on ice for 2 min (Ferroni *et al.*, 2014) or with 2% (w/v) digitonin at room temperature for 10 min under gentle agitation (Järvi *et al.*, 2011). To allow the best separation of large super- and megacomplexes, native complexes were separated using lpBN-PAGE as described by Järvi *et al.* (2011). For 2D separation of the individual protein subunits, the lpBN-PAGE strips were incubated for 1 h at 21°C in Laemmli buffer containing 5% (v/v) 2-mercaptoethanol (Laemmli, 1970) and subsequently analysed by SDS-PAGE and silver staining. Band intensity in lpBN lanes was quantified using ImageJ freeware (National Institutes of Health, Bethesda, MD, USA).

Chlorophyll fluorescence

Modulated Chl fluorescence was analysed with an ADC OS1-FL portable PAM fluorometer (ADC Bioscientific Ltd, Hoddesdon, UK). Samples were dark-acclimated for 30 min before recording induction curves under white actinic light of 1600 μmol m^{-2} s^{-1} brought to the sample through fibreoptics from a halogen lamp. Quantum yields of complementary processes were calculated according to Hendrickson *et al.* (2004) and corresponded to actual PSII photochemistry [Y(II)], regulated thermal dissipation [Y(NPQ)] and constitutive dissipation of heat and fluorescence [Y(NO)]. Fluorescence yields were combined for a synthetic comparison of general photochemical [Y(PSII)/Y(NO)] and nonphotochemical [Y(NPQ)/Y(NO)] capacities (Lazár, 2015). After induction as just described, the relaxation kinetics of Y(NPQ) was followed in darkness for 40 min in a semi-logarithmic plot to distinguish Y(NPQ) components differing in their decay times (Guadagno *et al.*, 2010). In *S. martensii*, Y(NPQ) decay was approximately biphasic, with a fast-relaxing component qE and a more slowly relaxing component qT, leaving an unrelaxed fraction qI (Ferroni *et al.*, 2014). The contribution of the three components to Y(NPQ) was calculated by fitting the relaxation curves with two exponential decays (qE and qT) and a constant (qI). The correctness of the Y(qI) value was checked by comparison with the residual difference between maximum PSII yield values (F_V/F_M) measured before and after the induction/relaxation protocol.

Single turnover fast fluorescence (FF) relaxation kinetics were measured using a double-modulation fluorometer (Photon System Instruments, Drasov, Czech Republic). Fluorescence decay kinetics in the range of 150 μs to 100 s were obtained, analysed and interpreted as described by Vass *et al.* (1999) and Allahverdiyeva *et al.* (2013).

The F730/F685 fluorescence ratio was calculated from normalized fluorescence emission spectra recorded at room temperature using a microspectrofluorimeter (RCS, Firenze, Italy) mounted on a Zeiss Axiophot microscope (excitation, 436 nm; Pancaldi *et al.*, 2002).

P700 redox state

PSI activity was analysed with a Walz Dual-PAM-100 (Heinz Walz GmbH, Effeltrich, Germany; Klughammer & Schreiber, 1994). After 30 min of dark acclimation, the maximum absorbance of $P700^+$ (P_M) was assessed according to the instrument instructions, applying a saturating pulse (6000 μmol m^{-2} s^{-1}; 300 ms) on top of far-red pre-illumination (720 nm wavelength; 191 μmol m^{-2} s^{-1}; 9 s duration). Light curves were subsequently recorded by exposing the sample to increasing actinic light (53–1594 μmol m^{-2} s^{-1}, each lasting 6 min). Steady-state (P) and maximum $P700^+$ absorbances in the light-acclimated state (P_M') were used to calculate the quantum yield of PSI photochemistry [Y(PSI)] and the complementary nonphotochemical yields corresponding to acceptor-side [Y(NA] and donor-side [Y(ND)] limitation of PSI. Notes S1 contains additional theoretical details.

Statistical analyses

One- or two-factor analysis of variance (ANOVA) was performed with OriginPro 2015 (OriginLab Corp., Northampton, MA, USA) (statistical significance at $P < 0.05$).

Results

Thylakoid architecture is heavily rearranged upon long-term light acclimation

Long-term light acclimation affected the angle of insertion of the ventral microphylls on the stem, which decreased from L to H plants (Fig. 1a–c). Far from the vein, the *S. martensii* leaf section is made up of three layers: large conical cells of the upper epidermis, a few sparse mesophyll cells, and lower epidermal cells. Leaf thickness in the section increased from L to H plants (Fig. 1d–f). In each leaf layer, cells contained chloroplasts, but the most relevant for photosynthesis was the single cup-shaped large chloroplast present in each upper epidermal cell. Upon long-term light acclimation, the organelle modulated the concavity of its top surface, from slightly convex in L plants to concave in M plants and markedly concave in H plants (Fig. 1g–i). Inside the chloroplast, the thylakoid system included two structurally different regions, which qualify the organelle as a 'bizonoplast', as described by Sheue *et al.* (2007) in *Selaginella erythropus.* In a typical bizonoplast, such as that in M plants (Fig. 1h), the upper zone of the thylakoid system has a lamellar architecture, consisting of long and parallel layers of appressed thylakoids (Fig. 1k), while the lower zone has a typical granal structure (Fig. 1n); when present,

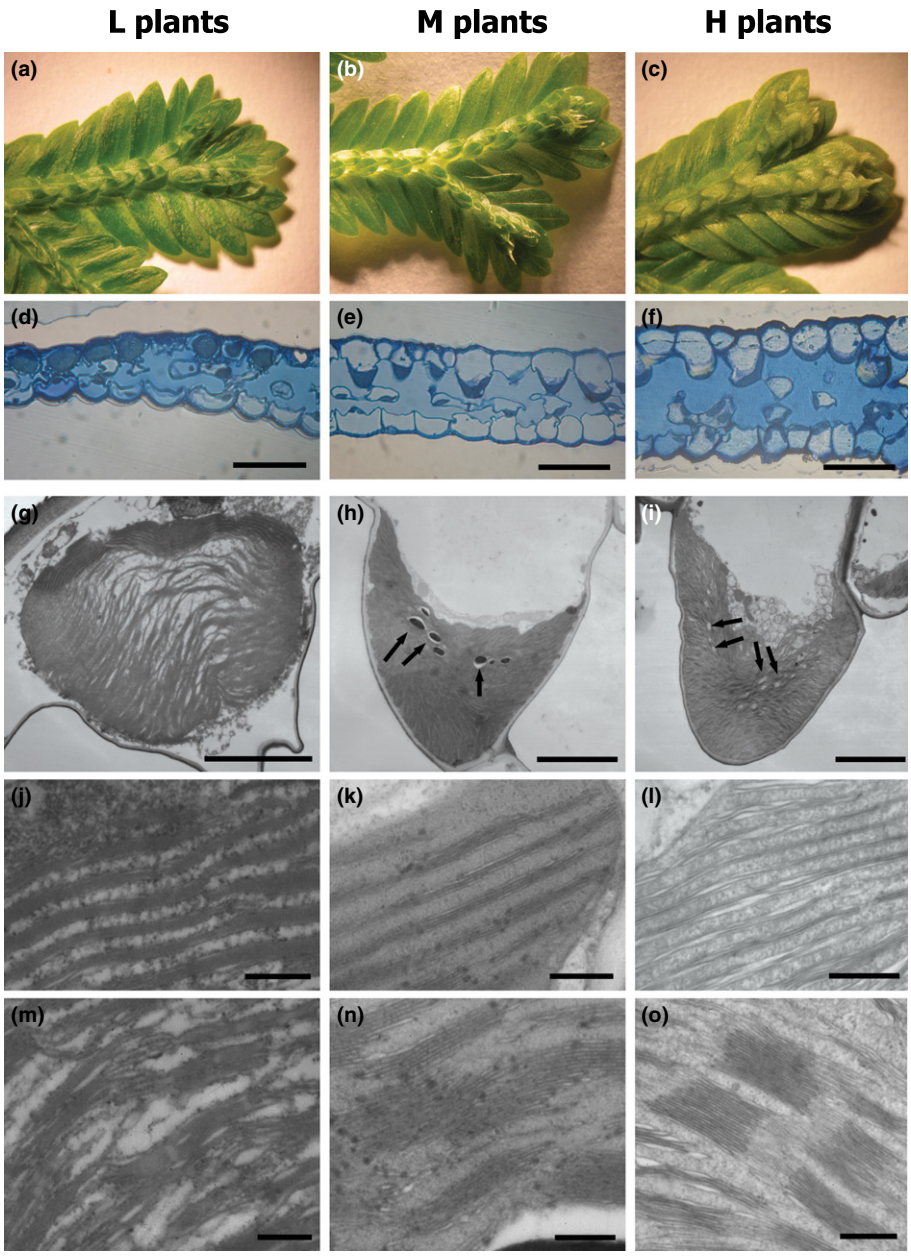

Fig. 1 Variations in leaf and chloroplast morphology in *Selaginella martensii* acclimated to different light regimes. (a–c) Terminal branches. (d–f) Light microscopy images of microphyll sections stained with toluidine blue; bars, 30 μm. (g–i) Chloroplast morphology in the upper epidermal cells; arrows indicate starch grains; bars, 5 μm. (j–l) Lamellar thylakoid arrangement in the upper zone of the thylakoid system; bars: (j, k) 0.25 μm; (l) 0.5 μm. (m–o) Lower zone of the thylakoid system, showing a pseudolamellar organization in low-light (L) plants (m) and a granal organization in medium-light (M) plants (n) and high-light (H) plants (o); bars, 0.25 μm.

starch grains were found mainly between the two zones (Fig. 1h). In L plants, the upper lamellae, each of which consisted of eight to 10 stacked thylakoids, appeared very dark because the membranes seemed to adhere at the lumenal side (Fig. 1j). The thylakoid lumen was, by contrast, easily recognizable in the thylakoids of M and particularly H plants, and a reduction in the number of stacked thylakoids per lamella was also clearly evident (Fig. 1k,l). In the lower thylakoid region, acclimation to extreme shade in L plants resulted in a thylakoid system with pseudolamellar organization, that is, a structure intermediate between the lamellar and granal structures, with only short connecting intergrana thylakoids (Fig. 1m). Similar to the upper zone, here the thylakoid lumen was not always evident. In M and H plants, by contrast, the granal structure of the lower region was typical, with variable degrees of stacking even inside the same organelle (Fig. 1n,o). The bizonoplasts of L plants did not store starch and had very clear stroma (Fig. 1g). In general, extreme shade promoted extensive stacking, resulting in a generalized (pseudo) lamellar organization, while in full sunlight the granal architecture prevailed over the lamellar architecture.

Relative amount of electron transport chain complexes, but not LHCII, is modulated depending on light regime

Sun/shade acclimation of the thylakoid membrane results primarily from changes in the relative amount of photosynthetic complexes, usually reflected by typical variations in pigment pattern. Amounts of Chl*a* and Chl*b* were very variable between different branches, with a nonsignificant decrease in H plants (Fig. 2a). The Chl*a*:*b* ratio increased very little from L to H and remained typical of shade plants even in H conditions (Fig. 2b). The total amount of carotenoids was also very variable, but

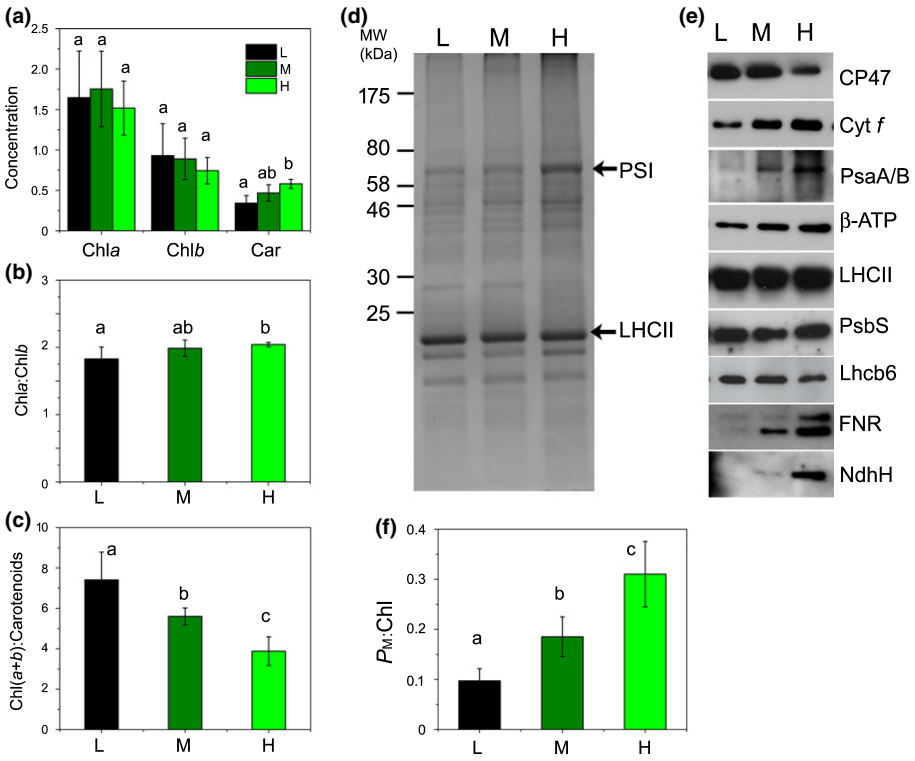

Fig. 2 Thylakoid composition in *Selaginella martensii* acclimated to different light regimes. Plants were analysed after long-term acclimation to a low (L), medium (M) or high (H) light regime. (a–c) Photosynthetic pigment content, expressed as nmol mg^{-1} FW (a) and as molar ratios of Chl*a* : Chl*b* (b) and Chl (*a* + *b*):carotenoids (c); data are mean ± 1SD with $n = 6$. (d) Denaturing electrophoresis (SDS-PAGE) profile of thylakoid proteins; samples were loaded on an equal Chl basis (1.5 μg) and the gel was stained with SYPRO Ruby; molecular marker on the left. (e) Immunoblot detection of thylakoid proteins separated by SDS-PAGE (1.5 μg of Chl loaded, with the exception of NAD(P)H dehydrogenase-like complex subunit H (NdhH) and ferredoxin-$NADP^+$ oxido-reductase (FNR), for the detection of which 2 μg of Chl was loaded). (f) Maximum photo-oxidizable photosystem I (PSI). The P_M value, obtained from $P700^+$ absorption signals, was normalized on the specific Chl content of each sample. Values are mean ± 1SD with $n = 4$. For each parameter, different letters indicate a significant difference between long-term acclimation conditions (one-factor ANOVA followed by *post hoc* Tukey's test; $P < 0.05$). A quantitative analysis of protein band intensities is reported in Supporting Information Fig. S2.

higher in H plants (Fig. 2a). In line with expectations, the Chl (*a* + *b*):carotenoid ratio markedly decreased from L to H plants (Fig. 2c; Lichtenthaler & Babani, 2004).

As the small variation in Chl*a*: *b* ratio apparently contrasted with the extensive restructuring of the thylakoid system, the thylakoid protein profile was first analysed with denaturing gels loaded on an equal Chl basis. When proteins were stained with the highly sensitive SYPRO Ruby, a fluorescent dye giving linear quantitative responses over a range of three orders of magnitude (Lopez *et al.*, 2000), two features were immediately evident: enrichment in PSI amount along the L-to-H gradient and invariability of the amount of LHCII (Fig. 2d). The increase in PSI content was independently confirmed by immunodetection of PsaA/B and through the determination of maximum photo-oxidizable PSI content, as the P_M value (Figs 2e,f, S2a). In immunoblots, increasing trends were also found for the Cyt*f* subunit of the Cytb_6f complex and the ATP synthase β subunit. The amount of PSII, evaluated as the content of one of its internal Chl*a*-containing antennae, CP47, did not change between L and M plants, but decreased markedly in H plants. The amount of LHCII was confirmed not to change upon long-term acclimation. Lhcb6, forming the minor PSII antenna CP24, instead decreased in parallel to the PSII core complex along the light gradient. Similar to LHCII, negligible variations affected the PsbS protein, which regulates the transition of LHCII from the harvesting to the quenched state under high light (Figs 2e, S2b). The increase in the relative amount of PSI found in H plants suggested a higher availability of electrons to the stromal acceptors. In support of this inference, FNR was analysed and indeed a clear enrichment of FNR occurred from L to H plants. From FNR, electrons can be driven to the Calvin–Benson–Bassham cycle or, alternatively, can be recycled to the PQ pool. An NAD(P)H dehydrogenase-like complex (NDH) is known to work in close cooperation with PSI in the thylakoid membrane of higher plants to recover electrons from ferredoxin and recycle them to the PQ pool (for reviews, see Rumeau *et al.*, 2007; Shikanai, 2014). The absence of the NdhH signal in L plants and the very low signal in M plants could be a consequence of low antibody sensitivity. In spite of this, a specific and strongly up-regulated accumulation of NDH was evident in H plants (Fig. 2e).

Long-term acclimation modulates the degree of association of LHCII with PSII

The modulations in the relative amount of the electron flux complexes matched the general model of sun/shade acclimation.

However, in contrast to the model, the invariability of the amount of LHCII raised the question about the way H plants, in particular, could organize an LHCII size that potentially exceeded the light-harvesting need of PSII. To obtain information on the association of LHCII with photosystems, thylakoid protein complexes were separated by lpBN-PAGE, which is optimized for efficient resolution of large thylakoid complexes, and which was previously set up also for *S. martensii* (Järvi *et al.*, 2011; Ferroni *et al.*, 2014). The relatively stable PSII–LHCII supercomplexes residing in grana cores can be sufficiently preserved using DM as a mild solubilizing agent (Pagliano *et al.*, 2012).

A reference lpBN-PAGE was run using thylakoids of M plants maintained under their growth light and attribution of bands to specific complexes was based on a 2D lpBN/SDS-PAGE separation (Fig. 3a). Under these conditions, PSI and PSII dimers, as well as ATP synthase, nearly co-migrated. Bands with higher molecular masses than PSI and PSII dimers were denoted as supercomplexes. In Fig. S3, the band profile of *S. martensii* is compared with that of the model angiosperm *Arabidopsis thaliana*. In *A. thaliana*, four types of PSII supercomplexes were resolved and assigned to PSII core dimers associated with one to four LHCII trimers (C_2S, C_2S_2, C_2S_2M and $C_2S_2M_2$) (Caffarri *et al.*, 2009; Pietrzykowska *et al.*, 2014). In *S. martensii*, a PSI–LHCII 'state-transition-like' complex was migrating below the PSII–LHCII supercomplexes, in line with our previous data showing that, in *S. martensii,* DM solubilization also preserves some PSI–LHCII interactions (Ferroni *et al.*, 2014). A second evident band included PSI, PSII and LHCII, but had lower molecular mass than the C_2S_2 of *A. thaliana*, suggesting that this band arose from two co-migrating distinct complexes of PSI and PSII, each associated with LHCII (Fig. S3). Higher molecular mass supercomplexes, including PSII and/or PSI with LHCII, characterized the upper part of the gel (Fig. 3a). In the lower molecular mass region, LHCII occurred mainly as a free trimer, but also as an LHCII complex formed by trimeric LHCII associated with Lhcb6 (Ferroni *et al.*, 2014). The Cytb_6f migrated slightly faster than the PSII monomers and was revealed by spots assignable to its subunits PetA, PetC and PetD (Aro *et al.*, 2005).

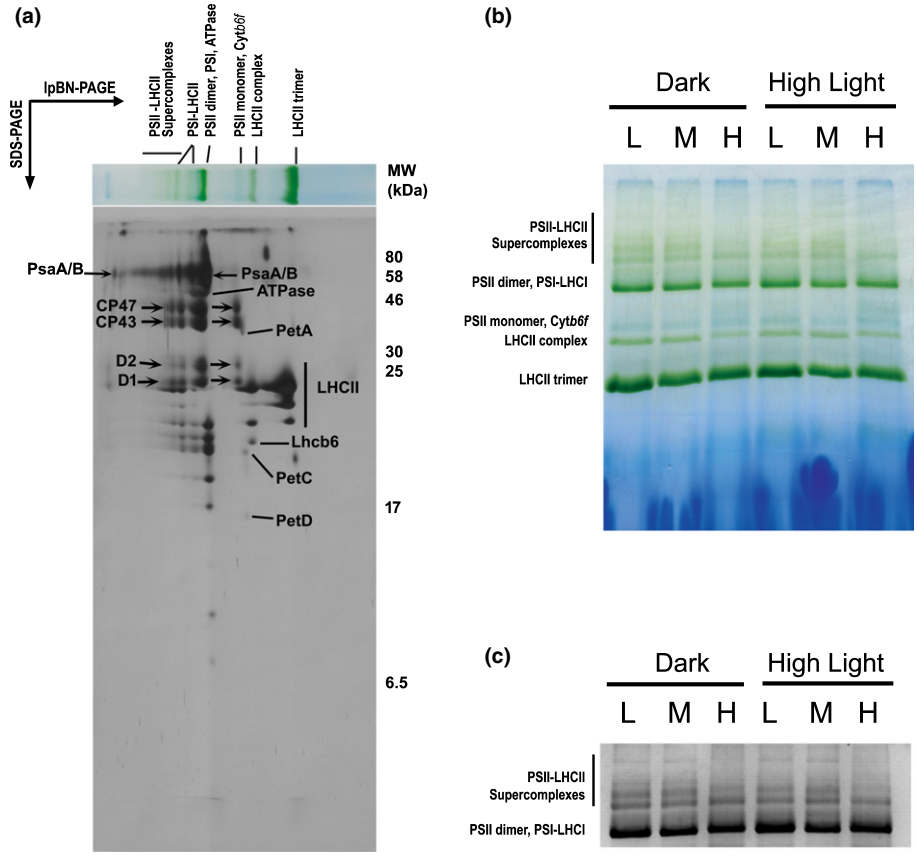

Fig. 3 Native thylakoid complexes of *Selaginella martensii* after solubilization with β-dodecylmaltoside (DM). (a) Reference silver-stained two-dimensional large-pore blue native/SDS polyacrylamide gel electrophoresis (lpBN/SDS-PAGE) of thylakoid complexes in medium light-grown (M) plants of *S. martensii* sampled under growth light conditions. Thylakoids at a Chl concentration of 0.5 mg ml^{-1} were solubilized with 1.5% DM and an lpBN gel was loaded with 6.5 μg of Chl. Assignment of spots to specific subunits is based on Ferroni *et al.* (2014) and Järvi *et al.* (2011): photosystem I (PSI), revealed by its subunits PsaA/B; photosystem II (PSII), revealed by its subunits D1, D2, CP43 and CP47; cytochrome b_6f (Cytb_6f), revealed by its subunits petA, petC and petD; ATP synthase (ATPase); major light-harvesting complex II (LHCII) and minor Lhcb6 antenna. The molecular marker is on the right. (b) lpBN-PAGE of thylakoids isolated from plants grown under different light regimes (L, low light; M, medium light; H, high light) after 12 h of dark incubation or 1 h of exposure to high light (1000 μmol m^{-2} s^{-1}). Solubilization and loading conditions were as in (a). (c) Upper portion of lpBN gel after staining with Coomassie brilliant blue to enhance band contrast. A quantitative analysis of band intensities is reported in Supporting Information Fig. S4.

Organization of thylakoid complexes was compared between plants in the dark-acclimated state and after 1 h of exposure to high light (Figs 3b, S4). Acclimation to darkness corresponds to a condition in which both membrane and stroma are in an oxidized state and the PSI–LHCII 'state-transition-specific' complexes characterizing low-light-acclimated plants are absent (Wientjes *et al.*, 2013b). In the case of *S. martensii*, the dark-acclimated state allowed analysis of PSII–LHCII supercomplexes without the interference of the co-migrating PSI–LHCII. The effects of the two variables, that is, 'long-term acclimation' and 'dark vs 1 h of high light', were tested with a two-factor ANOVA. Long-term acclimation significantly affected the abundance of PSII–LHCII supercomplexes, especially the highest molecular mass ones, and of the LHCII complex, all being less represented in H plants. The difference in the amount of supercomplexes was better visualized after staining the lpBN gels with Coomassie blue (Fig. 3c). The dark-to-high light transition did not cause statistically significant variations in the profiles of protein complexes. Interestingly, the bands corresponding to the free LHCII trimers and to co-migrating PSII dimers and PSI showed a constant abundance across all samples.

From extreme shade to high-light regime, plants increase their photochemical capacity while maintaining a high total capacity of thermal dissipation

It is well established that sun/shade acclimation usually impacts on the photochemical activity of PSII (Ballottari *et al.*, 2007; Anderson *et al.*, 2012; Zivcak *et al.*, 2014). PSII maximum yield, F_V/F_M, did not change between L, M and H plants (Fig. 4a). The use of light energy was compared during a 10-min-long exposure to high light. In all plants, the kinetics of Y(PSII) was characterized by a rapid decline during the first 30 s of exposure to high light (Fig. 4b). Subsequently, Y(PSII) showed a faster recovery in H plants (within 4 min) than in M plants (within 4 min), and only a limited recovery in L plants (Fig. 4c). This difference in kinetics was consistent with a gain in electron transport capacity from L to H plants (Tikhonov, 2015). Fig. 4(c) compares the use of light energy at the steady state in terms of complementary quantum yields (Hendrickson *et al.*, 2004). Steady-state Y(PSII) was lower in L plants than in M and H plants. Y(NO) comprises the yields of all nonregulatory dissipative processes, fluorescence emission included, and can also be used as a simple, though indirect, index of the reduction state of the PQ pool (Grieco *et al.*, 2012). Y(NO) was significantly lower in H plants, testifying to an enhanced ability to keep the PQ pool oxidized compared with L and M plants. Y(NPQ) did not differ between plants, which all relied on the capacity to safely dissipate > 60% of the absorbed light as heat. The Y(NPQ) : Y(NO) ratio, which equals Stern–Volmer-type NPQ, also confirmed an absence of significant variations (Fig. 4d). Conversely, the increase in the Y(PSII) : Y(NO) ratio provided straightforward evidence of the gain in overall photochemical capacity from L to H plants (Lazár, 2015; Fig. 4d).

Based on Y(PSII) kinetics and Y(PSII) : Y(NO), we hypothesized that long-term light acclimation could affect the pool of

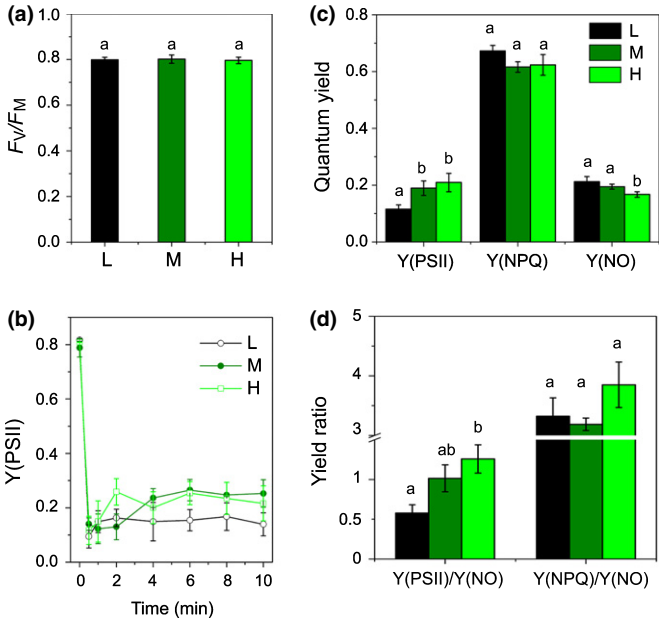

Fig. 4 Comparison of photosynthetic quantum yields in *Selaginella martensii* acclimated to different light regimes. Plants were analysed after long-term acclimation to a low (L), medium (M) or high (H) light regime. (a) Maximum photosystem II (PSII) quantum yield (F_V/F_M) after 30 min of dark acclimation. Values are mean ± 1SD ($n = 15$–18). (b) Slow induction kinetics of PSII yield [Y(PSII)] during irradiation with high light (1600 μmol m^{-2} s^{-1}); mean curves ± 1SD ($n = 3$). (c) Steady-state use of light energy in leaves treated for 10 min with high light. Quantum yields of energy conversion in PSII [Y(PSII)], regulatory thermal dissipation [Y(NPQ)] and constitutive energy loss [Y(NO)] were calculated as in Hendrickson *et al.* (2004). Y(NO) is also an index of the plastoquinone (PQ) reduction state (Grieco *et al.*, 2012). Values are mean ± 1SE ($n = 8$). (d) Yield ratios quantifying the total photochemical [Y(PSII)/Y(NO)] and thermal dissipation [Y(NPQ)/Y(NO)] capacity. Values are mean ± 1SE ($n = 8$). Different letters indicate a significant difference at $P < 0.05$, as determined using one-factor ANOVA followed by Tukey's test.

oxidized PQ available to re-open PSII after the reduction of the primary quinone electron acceptor of PSII (Q_A). FF relaxation profiles reflect the kinetics of dark re-oxidation of Q_A^- after reduction by a single-turnover light flash (Vass *et al.*, 1999). Three types of processes act together to re-oxidize Q_A^- (Vass *et al.*, 1999): (1) the fast (< 1-ms) forward electron transfer from Q_A^- to Q_B/Q_B^-, whose amplitude depends on the proportion of PSII containing a PQ molecule ready for reduction in the Q_B pocket before the flash; (2) the re-oxidation of Q_A^- by an oxidized PQ molecule moving from the PQ pool to the PSII that had an empty Q_B pocket at the moment of the flash, a process accomplished in some milliseconds; (3) the slow re-oxidation of Q_A^- by charge recombination with the oxygen evolving complex, occurring within seconds. FF relaxation kinetics were similar in M and H plants, but showed a slowdown in the middle portion of the curve obtained from L plants, indicating a limitation in the availability of oxidized PQ (Fig. 5; Table S1).

As Y(NPQ) is recognized as a composite of processes, different kinetic contributions were evaluated by analysing Y(NPQ) dark relaxation after high-light induction (Guadagno *et al.*, 2010). In a logarithmic plot of Y(NPQ) vs time, the first change in the

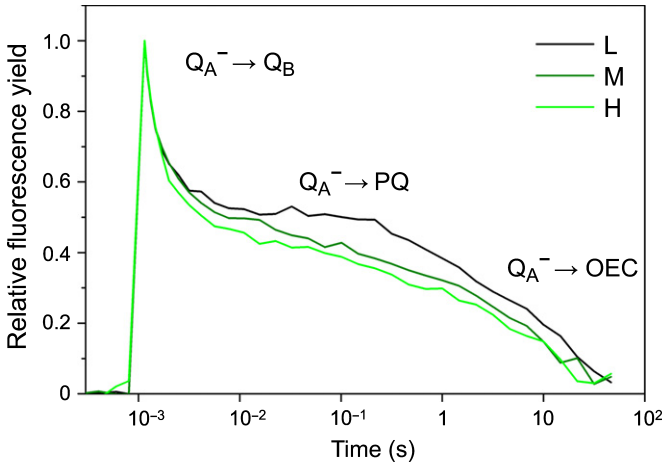

Fig. 5 Re-oxidation kinetics of the primary quinone electron acceptor of photosystem II (Q_A) in *Selaginella martensii* acclimated to different light regimes. Relaxation of single-turnover flash-induced Chl fluorescence yield was recorded for plants acclimated to a low (L), medium (M) or high (H) light regime. To allow comparison, relaxation curves were normalized between minimum and maximum fluorescences. Three processes contributing to the re-oxidation of Q_A are indicated at the approximate position of the curve where they occur: $Q_A^- \rightarrow Q_B$, forward electron transfer to the secondary quinone electron acceptor Q_B; $Q_A^- \rightarrow PQ$, forward electron transfer to a quinone molecule recruited from the plastoquinone (PQ) pool; $Q_A^- \rightarrow OEC$, charge recombination with the oxygen evolving centre (OEC) (see main text for further details and Supporting Information Table S1 for quantification of characteristic kinetic parameters). Each trace is the mean of four replicates.

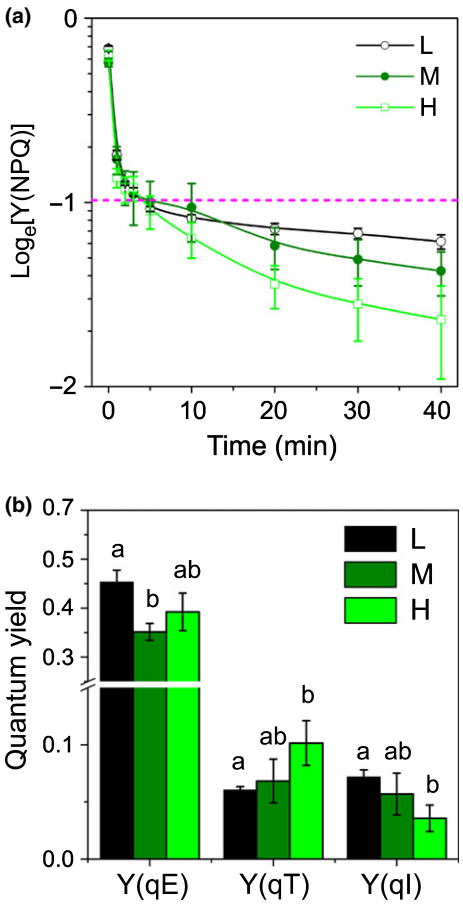

Fig. 6 Dark relaxation analysis of the yield of the regulatory thermal dissipation, [Y(NPQ)], induced in *Selaginella martensii*. Plants were analysed after long-term acclimation to a low (L), medium (M) or high (H) light regime. (a) Dark relaxation of the quantum yield of regulatory energy dissipation [Y(NPQ)] in plants previously exposed to 10 min of high light for induction (1600 μmol m^{-2} s^{-1}). The straight dashed line approximates the complete relaxation of the 'high-energy quenching' component (qE). (b) Quantum yields of qE [Y(qE)], more slowly relaxing [Y(qT)], and photoinhitory [Y(qI)] kinetic components, determined from Y(NPQ) relaxation curves. Values are means of four replicates ± 1SD. Different letters indicate significant difference at $P < 0.05$, as determined using ANOVA followed by Tukey's test.

slope corresponds to full relaxation of 'high-energy quenching' qE, which is the ΔpH-induced, carotenoid- and PsbS-dependent main de-excitation pathway in vascular plants (Demmig-Adams, 1990; Li *et al.*, 2000). Y(qE) was indeed the main fraction of Y (NPQ) in all samples. In spite of nearly overlapping curves, H samples showed somewhat faster relaxation ($t_{½}$ 27.1 s in H vs 31.2 s in L and 32.2 s in M; $P < 0.05$), while L plants had higher amplitudes (Fig. 6a,b). A relatively minor fraction of absorbed energy was funnelled into the de-excitation pathways responsible for the middle phase of Y(NPQ) relaxation, here indicated as qT (Fig. 6a,b). Imperfect logarithmic linearization of this phase was evidence for a complex origin; in fact, this kinetic component may arise from a mix of quenching processes relaxing with a $t_{½}$ of 10–15 min (see e.g. Kalaji *et al.*, 2014). Interestingly, the extent of Y(qT) was evidently dependent on long-term light acclimation, increasing along the light gradient (Fig. 6b). Finally, the residual, photoinhibitory component Y(qI) showed that H plants were the most resistant to photoinhibition, with their Y(qI) being half that of L plants (Fig. 6b).

The high-light-promoted physical interaction between PSI and LHCII does not necessarily result in enhanced energy distribution to PSI

We previously proposed that in *S. martensii* the qT developed upon high-light stress could depend on an LHCII-mediated photoprotective energy spillover to PSI (Ferroni *et al.*, 2014). Parallel trends of Y(qT) and PSI content suggested that long-term acclimation could also impact the labile PSI–LHCII interactions occurring in the stroma-exposed domains. Such interactions can be preserved using digitonin, a very mild detergent that solubilizes only stroma-exposed membranes, being unable to penetrate the compact structure of grana (Järvi *et al.*, 2011). A reference lpBN-PAGE was obtained from M plants under standard growth light (Fig. 7a). Based on the 2D separation of subunits and on comparative lpBN runs with *A. thaliana* (Figs 7a, S3; Suorsa *et al.*, 2015), the following complexes were identified with increasing molecular weight: LHCII free trimers; Cytb_6f migrating very close to a small amount of LHCII complex; PSII monomers; PSI approximately at the same height as ATP synthase and traces of PSII dimer; three individual complexes formed by PSI and LHCII (state transition-specific complexes); a nearly continuous 'train' of higher molecular mass non-state-

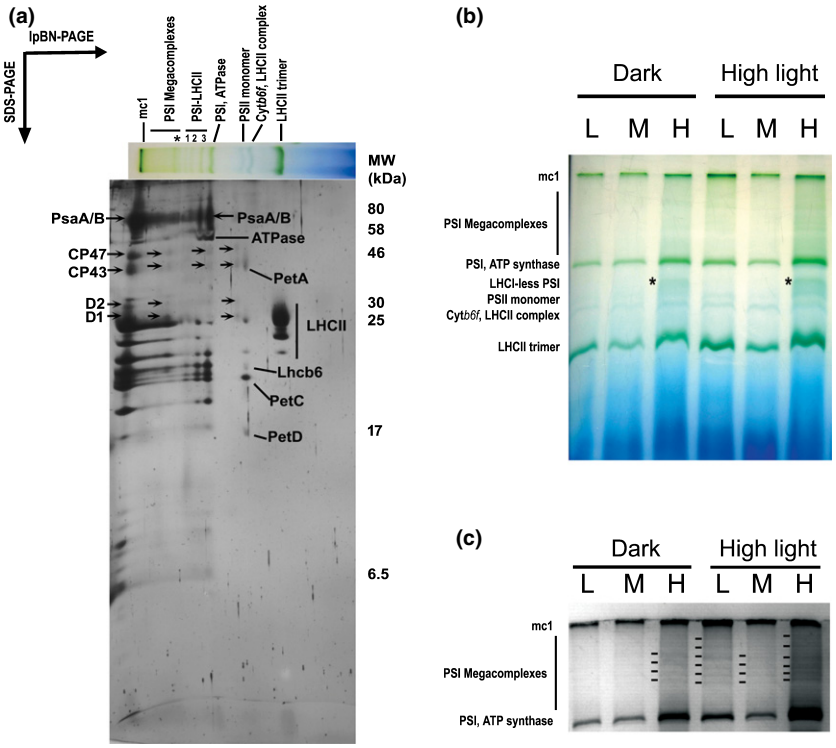

Fig. 7 Native complexes in stroma-exposed thylakoid domains of *Selaginella martensii* after solubilization with digitonin. (a) Reference silver-stained two-dimensional large-pore blue native/SDS polyacrylamide gel electrophoresis (lpBN/SDS-PAGE) of protein complexes in stroma-exposed thylakoids of *S. martensii* grown in medium light (M) conditions. Thylakoid aliquots containing 7.5 μg of Chl were solubilized with 2% digitonin at a Chl concentration of 0.5 mg ml^{-1}. Identification of spots is based on Järvi *et al.* (2011) and Suorsa *et al.* (2015): photosystem I (PSI), revealed by its subunits PsaA/B; photosystem II (PSII), revealed by its subunits D1, D2, CP43 and CP47; cytochrome b_6f (Cytb_6f), revealed by its subunits petA, petC and petD; ATP synthase (ATPase); major light-harvesting complex II (LHCII) and minor Lhcb6 antenna. The molecular marker is on the right. At high molecular weight, three individual complexes migrating more slowly than PSI were assigned to state-transition complexes (LHCII–PSI complexes 1, 2, and 3); note that the same LHCII–PSI state-transition complexes were resolved also in the lpBN gel after β-dodecylmaltoside (DM) solubilization, where they co-migrated with PSII–LHCII supercomplexes (see Fig. 3a). Heavier complexes are sustained by more labile interactions, not preserved with DM (see Fig. 3), and comprise PSI and LHCII (PSI megacomplexes). Asterisks mark a megacomplex containing also PSII. An extremely large PSI–LHCII–PSII megacomplex, mc1, was found just entering the resolving gel. (b) lpBN-PAGE of thylakoids isolated from plants grown under different light regimes (L, low light; M, medium light; H, high light) after 12 h of dark incubation or 1 h of exposure to high light (1600 μmol m^{-2} s^{-1}). As compared to the reference gel in (a), note that all samples lack individual bands corresponding to PSI–LHCII state-transition complexes. A band corresponding to LHCI-less PSI units is marked in H samples with an asterisk. (c) Upper portion of lpBN gel after staining with Coomassie brilliant blue to enhance band contrast. Individual PSI megacomplexes are marked with a dash.

transition megacomplexes containing PSI, LHCII and, in some cases, also a small amount of PSII; and an extremely large mega-complex, just entering the separation gel and formed by PSI, PSII and LHCII (Yokono *et al.*, 2015). Following the nomenclature proposed by Suorsa *et al.* (2015), this complex is indicated as mc1.

The lpBN profiles of the digitonin-solubilized complexes were examined with respect to the two variables 'long-term acclimation' and 'dark vs 1 h of high light' (Figs 7b, S5). All profiles lacked distinct bands of the state-transition complexes, characterizing instead the low-light acclimated condition (Fig. 7a; Wientjes *et al.*, 2013b). One band clearly resolved only in H thylakoids corresponded to LHCI-less PSI cores (Figs 7b, S6). In general, more complexes solubilized from H thylakoids (Fig. 7b,c). In fact, long-term acclimation significantly affected the amounts of PSI, Cytb_6f, PSII monomers and the non-state-transition PSI megacomplexes, but not mc1. Both PSI megacomplexes and mc1 accumulated upon a short-term exposure to high light, but, interestingly, the most marked accumulation of mc1 occurred in L plants (Fig. 7b,c).

As in angiosperms mc1 is currently believed to have a PSII photoprotective function through energy transfer from PSII to neighbouring PSI (Yokono *et al.*, 2015), we compared *S. martensii* plants with respect to PSI activity. Y(PSI) progressively declines upon increasing irradiance and the extent of such a decrease reflects the overall electron transport capacity (Fig. 8a). Comparison of Y(PSI) between M and H plants fully matched expectations, including an enhanced capacity of linear electron transport in H plants, which resulted in a higher peak of Y(NA) at low irradiance (Brestic *et al.*, 2015; Fig. 8c). Surprisingly, in L plants, Y(PSI) actually overlapped or was even higher than that of M plants (Fig. 8a). This result apparently contrasted with all other biochemical and fluorescence analyses, indicating instead L < M < H photochemical capacity. Complementary Y(ND) and Y(NA) also overlapped between L and M plants (Fig. 8b,c). Based on the methodological note reported in Notes S1, in L

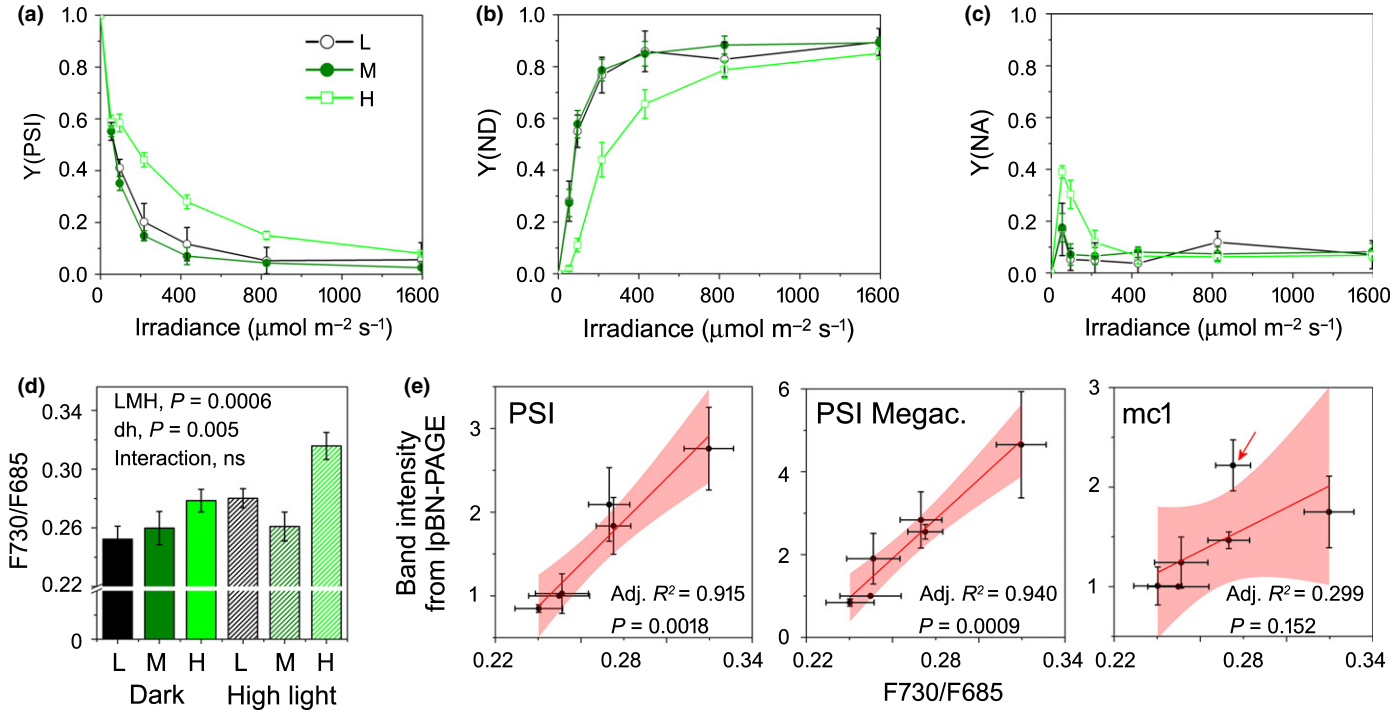

Fig. 8 Photosystem I (PSI) activity in *Selaginella martensii* acclimated to three light regimes. Plants were analysed after long-term acclimation to a low (L), medium (M) or high (H) light regime. Light curves of the complementary quantum yields of (a) PSI photochemistry Y(PSI), (b) nonphotochemical energy dissipation in donor-side limited PSI Y(ND), and (c) nonphotochemical energy dissipation in acceptor-side limited PSI Y(NA). Values are means of four replicates ± 1SD. (d) F730/F685 fluorescence emission ratio calculated from room-temperature emission spectra (see Supporting Information Fig. S7). Values are means of six to 11 replicates ± 1SE. Data were analysed with a two-factor ANOVA for the variables long-term acclimated condition (LMH) and dark vs high-light treated (dh) and their interaction. (e) Correlation analysis between F730/F685 and amount of PSI-containing complexes, as evaluated using lpBN-PAGE (see Figs 7, S5; mean value ± 1SE). The shaded area represents the 95% confidence interval. For the largest mc1 PSI–LHCII–PSII megacomplex, the outlier point indicated by the arrow corresponds to L plants exposed to 1 h of high light.

plants the trends of Y(PSI) and Y(ND) could be affected by a distortion caused by a quenched population of PSI, which was not reached by the excitation collected by the antenna system. Therefore, energy distribution between PSI and PSII was analysed in terms of F730/F685 fluorescence ratio, calculated from room-temperature emission spectra (Figs 8d, S7). Long-term acclimation and exposure to high light had a very significant influence on the energy distribution to PSI. The pattern of F730/F685 variation was compared with that of the PSI-containing complexes solubilized with digitonin and resolved by lpBN-PAGE (Figs 7b, S5). Correlation was very significant with PSI and PSI megacomplexes, but surprisingly not with mc1 (Fig. 8e). In particular, in the mc1 vs F730/F685 plot there was an evident outlier point, corresponding to the mc1 complex accumulated in L plants upon short-term high-light exposure. In the absence of this point, the amount of mc1 would correlate with F730/F685 with adjusted $R^2 = 0.861$ and $P = 0.015$. Therefore, high-light-treated L plants accumulated too much mc1 as compared to their actual gain in energy distribution to PSI.

Discussion

Modulability of the Chl*a*: *b* ratio and the amount of LHCII upon sun/shade acclimation is not a universal property of all land plants. The bryophytes lack this capability (Marschall & Proctor, 2004; Gerotto *et al.*, 2011) and, as is shown in this study, so does the lycophyte *S. martensii* (Fig. 2). *Selaginella martensii* is capable of modifying the leaf morphology and of regulating the amount of thylakoid membrane protein complexes and, consequently, the energy conversion capacity. More specifically, acclimation to higher light intensities markedly increased the amounts of protein complexes known to reside in nonappressed membranes, that is, PSI, ATP synthase, Cytb_6f and NDH (Fig. 2). The amount of PSII, in turn, was higher in plants acclimated to low light intensity.

As in angiosperms, in *S. martensii* only a minor part of LHCII is engaged in forming stable supercomplexes with PSII in the stacked domains of thylakoids, while the major part is found in the form of free trimers released upon DM or digitonin solubilization (Järvi *et al.*, 2011; Pagliano *et al.*, 2012; Ferroni *et al.*, 2014). In *A. thaliana*, long-term acclimation to high light mainly reduces the PSII-associated LHCII proteins, that is, Lhcb1-3 of the M trimers and the minor antenna protein Lhcb6 (Kouřil *et al.*, 2013; for Lhcb6, see also Ballottari *et al.*, 2007). Such LHCII composition limits the possibility of assembling supercomplexes larger than C_2S_2 (Kouřil *et al.*, 2013). A lower amount of $C_2S_2M_{(2)}$ manifests itself also as a decrease in the LHCII complexes, that is, M trimer/Lhcb6/Lhcb4 units (Wientjes *et al.*, 2013a). A comparable down-regulation of Lhcb6 occurred in H plants of *S. martensii*, leading to less abundant, smaller PSII units

(Figs 2e, 3b, S4). However, such fine-tuning occurs in the framework of an invariable free LHCII matrix. We decided to look beyond interactions involving merely PSII to better understand the location and role of the free LHCII. While the physiological importance of PSI–LHCII interactions has been known for decades in the context of short-term responses to changes in light quality ('state transitions'; for a review, see Goldschmidt-Clermont & Bassi, 2015), growing evidence indicates the relevance of LHCII interactions with both photosystems as a crucial acclimation mechanism. As the amount of PSI-binding LHCII in state-transition complexes is small compared with the abundant free LHCII trimers, Grieco *et al.* (2015) demonstrated that the LHCII lake mediates a more extensive connectivity between PSI and PSII at the grana margins, which can be revealed by non-state-transition, high-molecular-mass PSI–LHCII(–PSII) megacomplexes in digitonin-soluble thylakoid fractions (Järvi *et al.*, 2011). Whether it is technically possible to discriminate between native interactions and mere aggregation has been questioned, especially for the heaviest mc1 (Galka *et al.*, 2012), which nevertheless undergoes light-dependent regulation (Grieco *et al.*, 2015; Suorsa *et al.*, 2015; Yokono *et al.*, 2015). Interestingly, light acclimation responses of *S. martensii* strongly support a controlled accumulation of such PSI megacomplexes.

Sheue *et al.* (2007, 2015) reported that in *S. erythropus* the bizonoplast differentiation depends on light direction and intensity and, in particular, the upper lamellar zone represents an adaptation to deep shade. The generalized (pseudo)lamellar thylakoid organization in L plants of *S. martensii* supports those observations (Fig. 1g). In L plants, the assembly of larger PSII units is indeed consistent with the most recent understanding of thylakoid shade acclimation, which also includes a primary location of free LHCII in stacked domains (Fig. 3b; Wientjes *et al.*, 2013a; Kouřil *et al.*, 2013; Ware *et al.*, 2015). Interestingly, and in contrast to M plants, remodelling of the thylakoid architecture in L plants occurs without remarkable changes in LHCII/PSII stoichiometry (Fig. 2e). This observation can be explained by assuming a denser packing of LHCII and PSII in the membrane, which can result in a hindered transfer of excitons (Haferkamp *et al.*, 2010), hindered lateral mobility of plastocyanin in a shrunken thylakoid lumen (Kirchhoff *et al.*, 2011), slower diffusion of PQ (Kirchhoff *et al.*, 2000), and limited formation of PQH_2 because of slow proton diffusion through the interthylakoid gap (Tikhonov, 2015). Slowed Q_A re-oxidation (Fig. 5), limited electron transport (Fig. 4b,d) and an extremely narrow thylakoid lumen (Fig. 1j,m) can all be consequences of membrane overcrowding in L plants. This would also indicate that the transition from lamellar to granal organization may depend, among other factors, on a less dense protein packing from L to H conditions, finally resulting in a less strict lateral heterogeneity. How this can be controlled *in vivo* remains to be elucidated, but certain structural and functional analogies between the thylakoid (pseudo)lamellae of *S. martensii* and the 'pseudograna' described in *A. thaliana* CURVATURE THYLAKOID1 (CURT1) mutants suggest that factors regulating thylakoid curvature at the grana margins could play a significant role (Armbruster *et al.*, 2013).

In DM lpBN gels, not only the band of free LHCII but also that of co-migrating PSII dimers and PSI monomers remained stable despite different light environments (Fig. 3b). The maintenance of a relatively constant amount of LHCII and LHCII:(PSI+PSII) ratio (Figs 2, S4) is not predictable from the current long-term acclimation model suggested for angiosperms (Anderson *et al.*, 2012). In *S. martensii*, free LHCII can apparently serve a fixed proportion of reaction centres, either PSII or PSI, suggesting a flexible association of LHCII with both photosystems. Interestingly, the LHCII association balance appears to shift to PSI upon short-term high-light exposure, leading to the accumulation of mc1 and other high-molecular-mass PSI–LHCII megacomplexes (Figs 7b, S5). Conversely, the lighter state-transition-type PSI–LHCII complexes do not participate in the response to high light, confirming that their relevance for regulation of energy distribution is specific to low light conditions (Wientjes *et al.*, 2013b; Mekala *et al.*, 2015; Fig. 7a). We propose that the accumulation of heavy PSI–LHCII(–PSII) megacomplexes provides instead a specific benefit to *S. martensii* in conditions of excess light excitation.

We previously suggested that the 'high-light qT' induced in lycophytes reflects the occurrence of a photoprotective energy spillover from PSII to PSI (Ferroni *et al.*, 2014). In spite of an unclear, possibly multifactorial origin of this NPQ component in angiosperms (Demmig & Winter, 1988; Horton & Hague, 1988; Lokstein *et al.*, 1994; Schansker *et al.*, 2006; Joliot & Finazzi, 2010; Nilkens *et al.*, 2010; Cazzaniga *et al.*, 2013), in *S. martensii* its assignment to a PSI-based quenching mechanism is supported by its evident correlation with the PSI amount (Fig. 2d,f). Quenching of excess energy by PSI is probably especially relevant in H plants. More abundant FNR can drive electrons downstream to the stromal acceptors, allowing a high Y(PSI), and the specific accumulation of the NDH-like complex also provides an additional safety valve against an over-reduced electron transport chain (Figs 2e, 8a; Rumeau *et al.*, 2007; Shikanai, 2014). The use of PSI as an energy quencher for PSII requires that a certain fraction of energy harvested by LHCII is 'stolen' from PSII and re-directed to PSI. Based on the results obtained in *A. thaliana* by Yokono *et al.* (2015) and Suorsa *et al.* (2015), mc1 in particular can provide an ideal supramolecular environment where the excitation energy reaching the closed-state PSII can be effectively diverted to PSI. In H plants exposed to high light, an accumulation of mc1, but also of other high-molecular-mass non-state-transition PSI–LHCII(–PSII) megacomplexes, was indeed observed and was accompanied by a gain in energy distribution to PSI (Figs 7c, 8e). Even though the megacomplex interactions seem loosely cohesive after digitonin solubilization and lpBN electrophoresis, they are presumably more coherent *in vivo* and possibly involve almost all PSI units, as indicated by the positive correlation between F730/F685 and the PSI–LHCI core band (Fig. 8e).

The response to high light of *S. martensii* L plants provides further insight into the significance of mc1 in photoprotection. Here, a large accumulation of mc1 occurred, but resulted neither in high Y(qT) nor in a proportional gain in energy distribution to PSI (Figs 6b, 8e). These findings, along with otherwise

inexplicable distortions in Y(PSI) and Y(ND) determination (Fig. 8a,b), strongly suggest that a population of PSI embedded in mc1 is in a quenched state, that is, has been excluded from the excitation pathways. According to recent evidence, a very low content of PSI, such as that characterizing L plants, can further make PSI, not PSII, more prone to photodamage (Brestic *et al.*, 2015). However, PSI can be preserved by the activation of quenching mechanisms, which can involve zeaxanthin formation directly in LHCI (Ballottari *et al.*, 2014) or the quenching potential (qE) of the whole LHCII lake interspersed between PSI and PSII (Tikkanen & Aro, 2014). In *S. martensii*, the qE-related PsbS protein was present in stable amounts despite different light conditions (Fig. 2e), in striking contrast with the growth light-dependent PsbS accumulation described in angiosperms and in the moss *Physcomitrella patens* (Tikkanen *et al.*, 2006; Ballottari *et al.*, 2007; Gerotto *et al.*, 2011). As PsbS is a component of the megacomplexes (Suorsa *et al.*, 2015), it is very likely that LHCII can sustain, through PsbS, the quenching of PSI in mc1. In L plants, PSII photoprotection is also ensured through the cooperation of different mechanisms, beside qE. For instance, in the appressed domains, a possibly lower connectivity of PSII units could facilitate PSII protection, according to a hypothesis recently put forward by Zivcak *et al.* (2014). Moreover, in non-appressed membranes, PSII can still benefit from a certain capacity for energy spillover to PSI, which is apparently retained by PSI–LHCII–PSII megacomplexes of lower molecular mass than mc1 (Fig. 8e). As a consequence, PSII photoinhibition is kept under control, despite the plant's acclimation to extreme shade (Fig. 6b).

Conclusions

Long-term light acclimation requires a set of changes that safeguard a synergetic regulation of light harvesting and energy conversion (Lichtenthaler & Babani, 2004; Anderson *et al.*, 2012). In contrast to angiosperms, the regulation of light harvesting in the lycophyte *S. martensii* does not occur through variations in the relative amount of free LHCII, but results from the flexibility of the free LHCII association with both PSII and PSI. We propose that the regulation of PSI–LHCII (–PSII) megacomplexes is an integral part of long-term acclimation. Upon short-term high-light exposure, the interspersed free LHCII ensures photoprotection of PSII through qE, allows regulated use of PSI as an energy quencher, and can even quench endangered PSI. In view of this high complexity, the thylakoid organization in the bizonoplast cannot properly be considered as a primitive trait that would have been lost in more derived lineages of vascular plants, as was recently proposed (Sheue *et al.*, 2015). The nearly invariable grana–intergrana thylakoid arrangement in the angiosperm chloroplast (Solymosi & Keresztes, 2012) and the highly modulable thylakoid architecture in the bizonoplast of *Selaginella* could instead be two independent evolutionary outcomes in divergent lineages of vascular plants.

Acknowledgements

This research was supported by the University of Ferrara and the Academy of Finland (project nos. 271832 and 273870), TEKES LIF 40128/14, and the Initial Training Networks (ITN) CALIPSO (607607) and PHOTOCOMM (317184). L.F. acknowledges Erasmus Staff Teaching Assignment fellowships granted through the University of Ferrara in the academic years 2012/2013 and 2013/2014.

Author contributions

L.F. conceived and planned the research. L.F., M.S. and C.B. performed experiments. L.F., M.S., E-M.A. and S.P. analysed and interpreted data; L.F. wrote the manuscript with M.S. and S.P.

References

Allahverdiyeva Y, Suorsa M, Rossi F, Pavesi A, Kater MM, Antonacci A, Tadini L, Pribil M, Schneider A, Wanner G *et al.* 2013. *Arabidopsis* plants lacking PsbQ and PsbR subunits of the oxygen-evolving complex show altered PSII super-complex organization and short-term adaptive mechanisms. *The Plant Journal* **75**: 671–684.

Anderson JM, Chow WS, Goodchild DJ. 1988. Thylakoid membrane organization in sun/shade acclimation. *Australian Journal of Plant Physiology* **15**: 11–26.

Anderson JM, Horton P, Kim E-H, Chow WS. 2012. Towards elucidation of dynamic structural changes of plant thylakoid architecture. *Philosophical transactions of the Royal Society of London. Series B, Biological Sciences* **367**: 3515–3524.

Andersson B, Anderson JM. 1980. Lateral heterogeneity in the distribution of chlorophyll–protein complexes of the thylakoid membranes of spinach chloroplasts. *Biochimica et Biophysica Acta* **593**: 427–440.

Armbruster U, Labs M, Pribil M, Viola S, Xu W, Scharfenberg M, Hertle AP, Rojahn U, Jensen PE, Rappaport F *et al.* 2013. *Arabidopsis* CURVATURE THYLAKOID1 proteins modify thylakoid architecture by inducing membrane curvature. *The Plant Cell* **25**: 2661–2678.

Aro EM. 1982. A comparison of the chlorophyll-protein composition and chloroplast ultrastructure in two bryophytes and two higher plants. *Zeitschrift für Pflanzenphysiologie* **108**: 97–105.

Aro EM, Suorsa M, Rokka A, Allahverdiyeva Y, Paakkarinen V, Saleem A, Battchikova N, Rintamäki E. 2005. Dynamics of photosystem II: a proteomic approach to thylakoid protein complexes. *Journal of Experimental Botany* **56**: 347–356.

Baldisserotto C, Ferroni L, Anfuso E, Pagnoni A, Fasulo MP, Pancaldi S. 2007. Responses of *Trapa natans* L. floating laminae to high concentrations of manganese. *Protoplasma* **231**: 65–82.

Ballottari M, Alcocer MJP, D'Andrea C, Viola D, Ahn TK, Petrozza A, Polli D, Fleming GR, Cerullo G, Bassi R. 2014. Regulation of photosystem I light harvesting by zeaxanthin. *Proceedings of the National Academy of Sciences, USA* **111**: E2431–E2438.

Ballottari M, Dall'Osto L, Morosinotto T, Bassi R. 2007. Contrasting behavior of higher plant photosystem I and II antenna systems during acclimation. *Journal of Biological Chemistry* **282**: 8947–8958.

Bischof K, Rautenberger R, Brey L, Pérez-Lloréns JL. 2006. Physiological acclimation to gradients of solar irradiance within mats of the filamentous green macroalga *Chaetomorpha linum* from southern Spain. *Marine Ecology Progress Series* **306**: 165–175.

Brestic M, Zivcak M, Kunderlikova K, Sytar O, Shao H, Kalaji HM, Allakhverdiev SI. 2015. Low PSI content limits the photoprotection of PSI and PSII in early growth stages of chlorophyll b-deficient wheat mutant lines. *Photosynthesis Research* **125**: 151–166.

Caffarri S, Kouřil R, Kereiche S, Boekema EJ, Croce R. 2009. Functional architecture of higher plant photosystem II supercomplexes. *EMBO Journal* **28**: 3052–3063.

Cazzaniga S, Dall'Osto L., Kong S-G, Wada M, Bassi R. 2013. Interaction between avoidance of photon absorption, excess energy dissipation and zeaxanthin synthesis against photooxidative stress in *Arabidopsis*. *The Plant Journal* **76**: 568–579.

Demmig B, Winter K. 1988. Characterisation of three components of non-photochemical fluorescence quenching and their response to photoinhibition. *Australian Journal of Plant Physiology* **163**: 163–177.

Demmig-Adams B. 1990. Carotenoids and photoprotection in plants: a role for the xanthophyll zeaxanthin. *Biochimica et Biophysica Acta* **1020**: 1–24.

Demmig-Adams B, Cohu CM, Muller O, Adams WW III. 2012. Modulation of photosynthetic energy conversion efficiency in nature: from seconds to seasons. *Photosynthesis Research* **113**: 75–88.

Ferroni L, Angeleri M, Pantaleoni L, Pagliano C, Longoni P, Marsano F, Aro EM, Suorsa M, Baldisserotto C, Giovanardi M *et al.* 2014. Light-dependent reversible phosphorylation of the minor photosystem II antenna Lhcb6 (CP24) occurs in lycophytes. *The Plant Journal* 77: 893–905.

Galka P, Santabarbara S, Khuong TTH, Degand H, Morsomme P, Jennings RC, Boekema EJ, Caffarri S. 2012. Functional analyses of the plant photosystem I–light-harvesting complex II supercomplex reveal that light-harvesting complex II loosely bound to photosystem II is a very efficient antenna for photosystem I in state II. *The Plant Cell* **24**: 2963–2978.

Gerotto C, Alboresi A, Giacometti GM, Bassi R, Morosinotto T. 2011. Role of PSBS and LHCSR in *Physcomitrella patens* acclimation to high light and low temperature. *Plant, Cell & Environment* **34**: 922–932.

Goldschmidt-Clermont M, Bassi R. 2015. Sharing light between two photosystems: mechanism of state transitions. *Current Opinion in Plant Biology* **25**: 71–78.

Grieco M, Suorsa M, Jajoo A, Tikkanen M, Aro EM. 2015. Light-harvesting II antenna trimers connect energetically the entire photosynthetic machinery – including both photosystems II and I. *Biochimica et Biophysica Acta* **1847**: 607–619.

Grieco M, Tikkanen M, Paakkarinen V, Kangasjärvi S, Aro EM. 2012. Steady-state phosphorylation of light-harvesting complex II proteins preserves photosystem I under fluctuating white light. *Plant Physiology* **160**: 1896–1910.

Grouneva I, Gollan PJ, Kangasjärvi S, Suorsa M, Tikkanen M, Aro EM. 2013. Phylogenetic viewpoints on regulation of light harvesting and electron transport in eukaryotic photosynthetic organisms. *Planta* **237**: 399–412.

Guadagno CR, Virzo de Santo A, D'Ambrosio N. 2010. A revised energy partitioning approach to assess the yields of non-photochemical quenching components. *Biochimica et Biophysica Acta* **1797**: 525–530.

Gunning BES, Schwartz OM. 1999. Confocal microscopy of thylakoid autofluorescence in relation to origin of grana and phylogeny in the green algae. *Australian Journal of Plant Physiology* **26**: 695–708.

Haferkamp S, Haase W, Pascal AA, Van Amerongen H, Kirchhoff H. 2010. Efficient light harvesting by photosystem II requires an optimized protein packing density in grana thylakoids. *Journal of Biological Chemistry* **285**: 17020–17028.

Hendrickson L, Furbank RT, Chow WS. 2004. A simple alternative approach to assessing the fate of absorbed light energy using chlorophyll fluorescence. *Photosynthesis Research* **82**: 73–81.

Hogewoning SW, Wientjes E, Douwstra P, Trouwborst G, van Ieperen W, Croce R, Harbinson J. 2012. Photosynthetic quantum yield dynamics: from photosystems to leaves. *The Plant Cell* **24**: 1921–1935.

Horton P, Hague A. 1988. Studies on the induction of chlorophyll fluorescence in isolated barley protoplasts IV. Resolution of non-photochemical quenching. *Biochimica et Biophysica Acta* **932**: 107–115.

Järvi S, Suorsa M, Aro EM. 2015. Photosystem II repair in plant chloroplasts — regulation, assisting proteins and shared components with photosystem II biogenesis. *Biochimica et Biophysica Acta* **1847**: 900–909.

Järvi S, Suorsa M, Paakkarinen V, Aro EM. 2011. Optimized native gel systems for separation of thylakoid protein complexes: novel super and mega-complexes. *Biochemical Journal* **439**: 207–214.

Joliot PA, Finazzi G. 2010. Proton equilibration in the chloroplast modulates multiphasic kinetics of nonphotochemical quenching of fluorescence in plants. *Proceedings of the National Academy of Sciences, USA* **107**: 12728–12733.

Kalaji HM, Schansker G, Ladle RJ, Goltsev V, Bosa K, Allakhverdiev SI, Brestic M, Bussotti F, Calatayud A, Dąbrowski P *et al.* 2014. Frequently asked questions about *in vivo* chlorophyll fluorescence: practical issues. *Photosynthesis Research* **122**: 121–158.

Kirchhoff H, Hall C, Wood M, Herbstová M, Tsabari O, Nevo R, Charuvi D, Shimoni E, Reich Z. 2011. Dynamic control of protein diffusion within the granal thylakoid lumen. *Proceedings of the National Academy of Sciences, USA* **108**: 20248–20253.

Kirchhoff H, Horstmann S, Weis E. 2000. Control of the photosynthetic electron transport by PQ diffusion in microdomains in thylakoids of higher plants. *Biochimica et Biophysica Acta* **1459**: 148–168.

Klughammer C, Schreiber U. 1994. An improved method, using saturating light pulses, for the determination of photosystem I quantum yield via $P700^+$-absorbance changes at 830 nm. *Planta* **192**: 261–268.

Kouřil R, Wientjes E, Bultema JB, Croce R, Boekema EJ. 2013. High-light vs. low-light: effect of light acclimation on photosystem II composition and organization in *Arabidopsis thaliana*. *Biochimica et Biophysica Acta* **1827**: 411–419.

Kramer DM, Johnson G, Kiirats O, Edwards GE. 2004. New fluorescence parameters for the determination of Q_A redox state and excitation energy fluxes. *Photosynthesis Research* **79**: 209–218.

Laemmli UK. 1970. Cleavage of structural proteins during the assembly of the head of bacteriophage T4. *Nature* **227**: 680–685.

Lazár D. 2015. Parameters of photosynthetic energy partitioning. *Journal of Plant Physiology* **175**: 131–147.

Li XP, Björkman O, Shih C, Grossman AR, Rosenquist M, Jansson S, Niyogi KK. 2000. A pigment-binding protein essential for regulation of photosynthetic light harvesting. *Nature* **403**: 391–395.

Lichtenthaler HK, Babani F. 2004. Light adaptation and senescence of the photosynthetic apparatus. Changes in pigment composition, chlorophyll fluorescence parameters and photosynthetic activity. In: Papageorgiou GC, Govindjee, eds. *Chlorophyll a fluorescence a signature of photosynthesis – advances in photosynthesis and respiration series, vol. 19*. Dordrecht, the Netherlands: Springer, 713–736.

Lokstein H, Härtel H, Hoffmann P, Woitke P, Renger G. 1994. The role of light-harvesting complex II in excess excitation energy dissipation: an *in vivo* fluorescence study on the origin of high-energy quenching. *Journal of Photochemistry and Photobiology B: Biology* **26**: 175–184.

Lopez MF, Berggren K, Chernokalskaya E, Lazarev A, Robinson M, Patton WF. 2000. A comparison of silver stain and SYPRO Ruby Protein Gel Stain with respect to protein detection in two-dimensional gels and identification by peptide mass profiling. *Electrophoresis* **21**: 3673–3683.

Marschall M, Proctor MCF. 2004. Are bryophytes shade plants? Photosynthetic light responses and proportions of chlorophyll *a*, chlorophyll *b* and total carotenoids. *Annals of Botany* **94**: 593–603.

Maxwell DP, Falk S, Huner NP. 1995. Photosystem II excitation pressure and development of resistance to photoinhibition. I. Light-harvesting complex II abundance and zeaxanthin content in *Chlorella vulgaris*. *Plant Physiology* **107**: 687–694.

Mekala NR, Suorsa M, Rantala M, Aro EM, Tikkanen M. 2015. Plants actively avoid state transitions upon changes in light intensity: role of light-harvesting complex II protein dephosphorylation in high light. *Plant Physiology* **168**: 721–738.

Murchie EH, Horton P. 1998. Contrasting patterns of photosynthetic acclimation to the light environment are dependent on the differential expression of the responses to altered irradiance and spectral quality. *Plant, Cell & Environment* **21**: 139–148.

Nasrulhaq-Boyce A, Duckett JG. 1991. Dimorphic epidermal cell chloroplasts in the mesophyll-less leaves of an extreme-shade tropical fern. *New Phytologist* **119**: 433–444.

Nasrulhaq-Boyce A, Haji MMA. 1987. Photosynthetic and respiratory characteristics of Malayan sun and shade ferns. *New Phytologist* **105**: 81–88.

Nevo R, Charuvi D, Tsabari O, Reich Z. 2012. Composition, architecture and dynamics of the photosynthetic apparatus in higher plants. *The Plant Journal* **70**: 157–176.

Nilkens M, Kress E, Lambrev P, Miloslavina Y, Müller M, Holzwarth AR, Jahns P. 2010. Identification of a slowly inducible zeaxanthin-dependent component of non-photochemical quenching of chlorophyll fluorescence generated under steady-state conditions in *Arabidopsis*. *Biochimica et Biophysica Acta* **1797**: 466–475.

Pagliano C, Barera S, Chimirri F, Saracco G, Barber J. 2012. Comparison of the α and β isomeric forms of the detergent n-dodecyl-D-maltoside for solubilizing photosynthetic complexes from pea thylakoid membranes. *Biochimica et Biophysica Acta* **1817**: 1506–1515.

Pancaldi S, Baldisserotto C, Ferroni L, Bonora A, Fasulo MP. 2002. Room-temperature microspectrofluorimetry as a useful tool for studying the assembly of the PSII chlorophyll-protein complexes in single living cells of etiolated *Euglena gracilis* Klebs during the greening process. *Journal of Experimental Botany* **53**: 1753–1763.

Pantaleoni L, Ferroni L, Baldisserotto C, Aro EM, Pancaldi S. 2009. Photosystem II organisation in chloroplasts of *Arum italicum* leaf depends on tissue location. *Planta* **230**: 1019–1031.

Pietrzykowska M, Suorsa M, Semchonok DA, Tikkanen M, Boekema EJ, Aro EM, Jansson S. 2014. The light-harvesting chlorophyll *a/b* binding proteins Lhcb1 and Lhcb2 play complementary roles during state transitions in *Arabidopsis*. *The Plant Cell* **26**: 3646–3660.

Porra RJ, Thompson WA, Kriedemann PE. 1989. Determination of accurate extinction coefficients and simultaneous equations for assaying chlorophyll a and chlorophyll b extracted with 4 different solvents – verification of the concentration of chlorophyll standards by atomic-absorption spectroscopy. *Biochimica et Biophysica Acta* **975**: 384–394.

Pribil M, Labs M, Leister D. 2014. Structure and dynamics of thylakoids in land plants. *Journal of Experimental Botany* **65**: 1955–1972.

Rumeau D, Peltier G, Cournac L. 2007. Chlororespiration and cyclic electron flow around PSI during photosynthesis and plant stress response. *Plant, Cell & Environment* **30**: 1041–1051.

Schansker G, Tóth SZ, Strasser RJ. 2006. Dark-recovery of the Chl *a* fluorescence transient (OJIP) after light adaptation: the qT component of non-photochemical quenching is related to an activated photosystem I acceptor side. *Biochimica et Biophysica Acta* **1757**: 787–797.

Sheue CR, Liu JW, Ho JF, Yao AW, Wu YH, Das S, Tsai CC, Chu HA, Ku MSB, Chesson P. 2015. A variation on chloroplast development: the bizonoplast and photosynthetic efficiency in the deep-shade plant *Selaginella erythropus*. *American Journal of Botany* **102**: 500–511.

Sheue CR, Sarafis V, Kiew R, Liu HY, Salino A, Kuo-Huang LL, Yang YP, Tsai CC, Lin CH, Yong JWH *et al.* 2007. Bizonoplast, a unique chloroplast in the epidermal cells of microphylls in the shade plant *Selaginella erythropus* (Selaginellaceae). *American Journal of Botany* **94**: 1922–1929.

Shikanai T. 2014. Central role of cyclic electron transport around photosystem I in the regulation of photosynthesis. *Current Opinion in Biotechnology* **26**: 25–30.

Solymosi K, Keresztes Á. 2012. Plastid structure, diversification and interconversions II. Land plants. *Current Chemical Biology* **6**: 186–204.

Song YZ, Gibbs SP. 1995. Photosystem I is not segregated from Photosystem II in the green alga *Tetraselmis subcordiformis*. *Protoplasma* **189**: 267–280.

Suorsa M, Rantala M, Danielsson R, Järvi S, Paakkarinen V, Schröder WP, Styring S, Mamedov F, Aro EM. 2014. Dark-adapted spinach thylakoid protein heterogeneity offers insights into the photosystem II repair cycle. *Biochimica et Biophysica Acta* **1837**: 1463–1471.

Suorsa M, Rantala M, Mamedov F, Lespinasse M, Trotta A, Grieco M, Vuorio E, Tikkanen M, Järvi S, Aro EM. 2015. Light acclimation involves dynamic re-organisation of the pigment-protein megacomplexes in non-appressed thylakoid domains. *The Plant Journal* **84**: 360–373.

Teramoto H, Nakamori A, Minagawa J, Ono TA. 2002. Light-intensity-dependent expression of Lhc gene family encoding light-harvesting chlorophyll-*a/b* proteins of photosystem II in *Chlamydomonas reinhardtii*. *Plant Physiology* **130**: 325–333.

Tikhonov AN. 2015. Induction events and short-term regulation of electron transport in chloroplasts: an overview. *Photosynthesis Research* **125**: 65–94.

Tikkanen M, Aro EM. 2014. Integrative regulatory network of plant thylakoid energy transduction. *Trends in Plant Science* **19**: 10–17.

Tikkanen M, Piippo M, Suorsa M, Sirpiö S, Mulo P, Vainonen J, Vener AV, Allahverdiyeva Y, Aro EM. 2006. State transitions revised – a buffering system for dynamic low light acclimation of *Arabidopsis*. *Plant Molecular Biology* **62**: 779–793.

Vass I, Kirilovsky D, Etienne AL. 1999. UV-B radiation-induced donor and acceptor-side modifications of photosystem II in the cyanobacterium *Synechocystis* sp. PCC 6803. *Biochemistry* **38**: 12786–12794.

Walters RG, Horton P. 1994. Acclimation of *Arabidopsis thaliana* to the light environment: changes in composition of the photosynthetic apparatus. *Planta* **195**: 248–256.

Ware MA, Belgio E, Ruban AV. 2015. Photoprotective capacity of non-photochemical quenching in plants acclimated to different light intensities. *Photosynthesis Research* **126**: 261–274.

Webb MR, Melis A. 1995. Chloroplast response in *Dunaliella salina* to irradiance stress (effect on thylakoid membrane protein assembly and function). *Plant Physiology* **107**: 885–893.

Wellburn AR. 1994. The spectral determination of chlorophyll-*a* and chlorophyll-*b*, as well as total carotenoids, using various solvents with spectrophotometers of different resolution. *Journal of Plant Physiology* **144**: 307–313.

Wientjes E, van Amerongen H, Croce R. 2013a. Quantum yield of charge separation in photosystem II: functional effect of changes in the antenna size upon light acclimation. *Journal of Physical Chemistry B* **117**: 11200–11208.

Wientjes E, van Amerongen H, Croce R. 2013b. LHCII is an antenna of both photosystems after long-term acclimation. *Biochimica et Biophysica Acta* **1827**: 420–426.

Wilk L, Grunwald M, Liao PN, Walla PJ, Kühlbrandt W. 2013. Direct interaction of the major light-harvesting complex II and PsbS in nonphotochemical quenching. *Proceedings of the National Academy of Sciences, USA* **110**: 5452–5456.

Wunder T, Xu W, Liu Q, Wanner G, Leister D, Pribil M. 2013. The major thylakoid protein kinases STN7 and STN8 revisited: effects of altered STN8 levels and regulatory specificities of the STN kinases. *Frontiers in Plant Science* **4**: 417.

Yamazaki J, Suzuki T, Maruta E, Kamimura Y. 2005. The stoichiometry and antenna size of the two photosystems in marine green algae, *Bryopsis maxima* and *Ulva pertusa*, in relation to the light environment of their natural habitat. *Journal of Experimental Botany* **56**: 1517–1523.

Yokono M, Takabayashi A, Akimoto S, Tanaka A. 2015. A megacomplex composed of both photosystem reaction centres in higher plants. *Nature Communications* **6**: 6675.

Zivcak M, Brestic M, Kalaji HM, Govindjee. 2014. Photosynthetic responses of sun- and shade-grown barley leaves to high light: is the lower PSII connectivity in shade leaves associated with protection against excess of light? *Photosynthesis Research* **119**: 339–354.

Supporting Information

Additional Supporting Information may be found online in the supporting information tab for this article:

Fig. S1 Diurnal variation in irradiance under the three light regimes, low light (L), medium light (M) and high light (H).

Fig. S2 Densitometric quantification of thylakoid protein bands.

Fig. S3 lpBN-PAGE profiles of thylakoids isolated from *Selaginella martensii* and the model angiosperm *Arabidopsis thaliana* under growth light conditions.

Fig. S4 Densitometric quantification of bands separated by lpBN-PAGE of DM-solubilized thylakoids.

Fig. S5 Densitometric quantification of bands separated by lpBN-PAGE of digitonin-solubilized thylakoids.

Fig. S6 Two-dimensional lpBN/SDS-PAGE of thylakoids isolated from *Selaginella martensii* H plants and solubilized with digitonin.

Fig. S7 Room-temperature fluorescence emission spectra.

Table S1 Characteristic kinetic parameters of the FF relaxation curves

Notes S1 Theoretical notes about the effect of a quenched PSI population on the determination of complementary PSI yields using the saturation pulse method.

Please note: Wiley Blackwell are not responsible for the content or functionality of any supporting information supplied by the authors. Any queries (other than missing material) should be directed to the *New Phytologist* Central Office.